Available online at www.sciencedirect.com
ScienceDirect
Materials Research Bulletin 43 (2008) 453–462
Materials Research Bulletin
www.elsevier.com/locate/matresbu

Raman characterization of boron doped tetrahedral amorphous carbon films

Manlin Tan *, Jiaqi Zhu, Jiecai Han, Wei Gao, Aiping Liu, Xiao Han

Center for Composite Materials, Harbin Institute of Technology, No. 2 Yikuang Street, Nangang District, Harbin 150001, China

Received 21 September 2006; received in revised form 7 January 2007; accepted 19 February 2007
Available online 1 March 2007

Abstract

Boron doped tetrahedral amorphous carbon films, having boron content from 0.59 to 6.04 at.%, have been prepared by a filtered cathodic vacuum arc system using boron mixed graphite targets. The influence of boron on the surface morphologies and microstructures of the films was studied by atomic force microscopy and Raman spectroscopy. The surface images showed that the irregular tops on the surface of the films tended to form larger clusters as boron content increased. The Raman spectra of the films were, respectively, deconvoluted using Gaussian and Breit–Wigner–Fano line shapes. The Raman parameters, including the intensity ratios, peak positions, peak widths and coupling coefficients, obtained from both line shapes were described and compared. It was found that both line shapes could produce consistent results except the peak widths of G bands. The major effect of boron introduction was to increase the clustering of the sp^2 phase in the films.

Keywords: A. Amorphous materials; A. Thin films; B. Vapor deposition; C. Raman spectroscopy; D. Microstructure

1. Introduction

Carbon films have evoked great interest for many years due to their versatile allotropes and physical properties arising from the adjustable ratio of sp^2 and sp^3 carbon hybridizations [1–3]. In general, an amorphous carbon can have any mixture of sp^3, sp^2, and even sp^1 sites, with the possible presence of up to 60 at.% hydrogen [3]. However, for a tetrahedral amorphous carbon (ta-C), it is often characterized by its high percentage (85%) of "diamond-like" sp^3 bonding [3]. In the past two decades, ta-C films have been intensively studied for their potential applications in surface coating [4,5] and field emission technology [6,7]. The attempt to incorporate boron into ta-C film has attracted many researchers to make it as a p-type semiconductor material [8–10]. However, there has been no agreed success on the preparation of p-type ta-C films. One important reason for this is that the p-type *doping* of ta-C films is not well characterized or understood [11].

Raman spectroscopy is a standard nondestructive tool for the characterization of crystalline, nanocrystalline, and amorphous carbon based materials [12]. The large differences of the Raman spectra in the various forms of carbon [12] allow it to be used to study the structural arrangements of the carbon atoms in ta-C films. By excitation with photons of visible light the Raman spectrum is dominated by scattering of sp^2-bonded graphitic carbon, due to resonance enhancement of the Raman scattering cross-section. For ta-C film, it has been concluded that the Raman spectrum is

* Corresponding author. Tel.: +86 451 86402954; fax: +86 451 86417970.
E-mail address: tanmanlin@yahoo.com.cn (M.L. Tan).

0025-5408/$ – see front matter © 2007 Published by Elsevier Ltd.
doi:10.1016/j.materresbull.2007.02.037

similar to that of microcrystalline graphite, which is overlaid by a G band at 1580–1600 cm^{-1} and a D band or shoulder around 1350 cm^{-1} [12,13]. In order to quantitatively analyze the Raman spectra, researchers have often used the decomposition method, which is sometimes called curve-fitting technique [14]. In the fit of the Raman spectra, two Gaussians or a combination of Breit–Wigner–Fano (BWF)/Lorentzian functions are often used for the deconvolution of G and D bands [12]. However, there exists some confusions associated with different trends of the Raman parameters under varying preparation conditions, due to the existence of the two different fitting procedures [15].

In this study, we report a Raman scattering study of boron doped tetrahedral amorphous carbon (ta-C:B) films prepared by filtered cathodic vacuum arc (FCVA) technique. The deconvolution of the Raman spectra by the two types of line-shape is described and compared. The Raman parameters, including the intensity ratios, peak positions, peak widths and coupling coefficients, are used to correlate the crucial role of incorporated boron. The aim is to give a detailed interpretation of the evolution of Raman spectra in terms of microstructure modifications for ta-C:B films.

2. Experimental

The films used in this study were deposited by a FCVA chamber. In the FCVA process, a double bend off-plane filter was used to remove the macroparticles and neutrals [16]. The cathodes were prepared using high-pure graphite mixed with 98% boron powder (with a small amount of Si), which was cool isostatically compressed as small disks under a pressure of 270 MPa for 6 min. The weight percentage of boron in the cathodes varied from 1% to 15%. N-type (1 1 1) silicon wafers were employed as the substrate. The wafers were cleaned in the acetone reagent using an ultrasonic machine before being placed in the vacuum chamber. A series of samples were then prepared at a constant bias $V_b = -80$ V using the cathodes with different boron concentrations.

The atomic percentage of B was identified in the range of 0.59–6.04 at.% by X-ray photoelectron spectroscopy (XPS) analysis using a PHI ESCA 5700 X-ray Photoelectron Spectrometer. The surface morphological characteristics of the films were measured by a Dimension 3100 atomic force microscopy (AFM). The stresses of the films were obtained by measuring the curvature of the Si substrates prior to or after deposition. The stress values could then be calculated using Stoney's formula.

The microstructure of the ta-C:B films was characterized by a Labram HR 800 Raman spectrometer (Jobin Yvon) whose wavelength of excited light source is 458 nm. In measurement, the laser beam was focused onto the sample surface using an optical microscope with a magnification of 50× (laser spot size ~1 μm). A low input power of 2 mW was used in order to minimize any possible beam heating effects, and the sampling duration was set to 60 s. The acquired Raman spectra in the range of 1100–1900 cm^{-1} were, respectively, deconvoluted with Gaussian lines and BWF lines to evaluate the difference in the structure of the films.

3. Results and discussion

3.1. Surface morphology

Fig. 1 shows the three-dimensional AFM images of B-doped and undoped ta-C films. The films in Fig. 1(a)–(c) were, respectively, with boron content of 0, 2.13 and 6.04 at.%. The thicknesses of the films were approximately 100 nm. The topography of ta-C film, shown in Fig. 1(a), contained very small and irregular tops separated by a large number of boundaries. While for the ta-C:B film in Fig. 1(b) the irregular tops have changed into homogeneous clusters, and a column-like structure is promoted. As the boron concentration increased up to 6.04 at.%, larger clusters could be seen for ta-C:B films in Fig. 1(c). The boundaries between the clusters of the film with 6.04 at.% boron became sparser than the film with boron content of 2.13 at.%. It should be point out that the dominant morphology size is not the crystallite size of the film. Thus it can be hypothesized that the fine clusters in the undoped ta-C film are due to a large percentage of sp^3 carbon bonding formed by the high impinging carbon energies [17], while the large clusters in ta-C:B films are due to the delocalizing of sp^2 sites after boron incorporation.

3.2. Raman line-shape of ta-C:B

The main feature in the Raman spectra of ta-C:B films is an asymmetric peak between 1100 and 1900 cm^{-1} centered at 1500–1570 cm^{-1} (Fig. 2), which is attributed to the vibrational mode of sp^2-bonded carbon clusters.

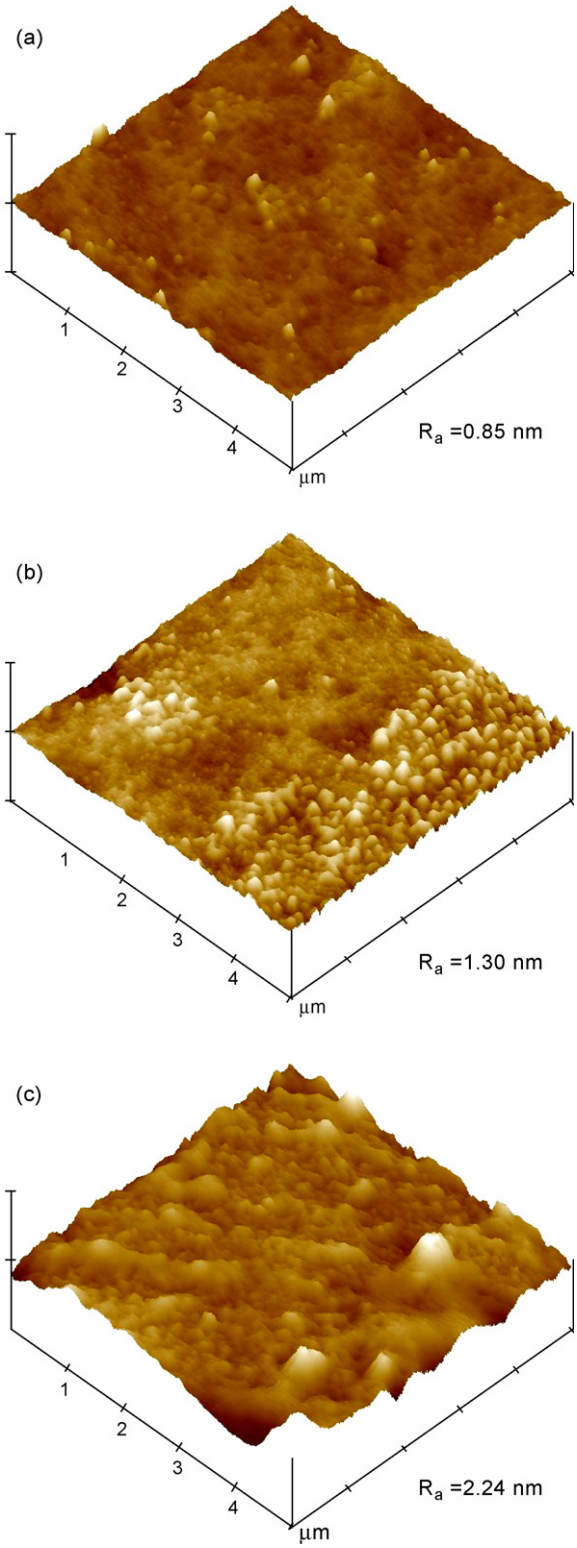

Fig. 1. Surface morphologies of: (a) ta-C film, (b) ta-C:B film with B content of 2.13 at.%, (c) ta-C:B film with B content of 6.04 at.%. The mean roughness (Ra) of each sample was also annotated. (X—1.000 μm/div, Z—50.000 nm/div.)

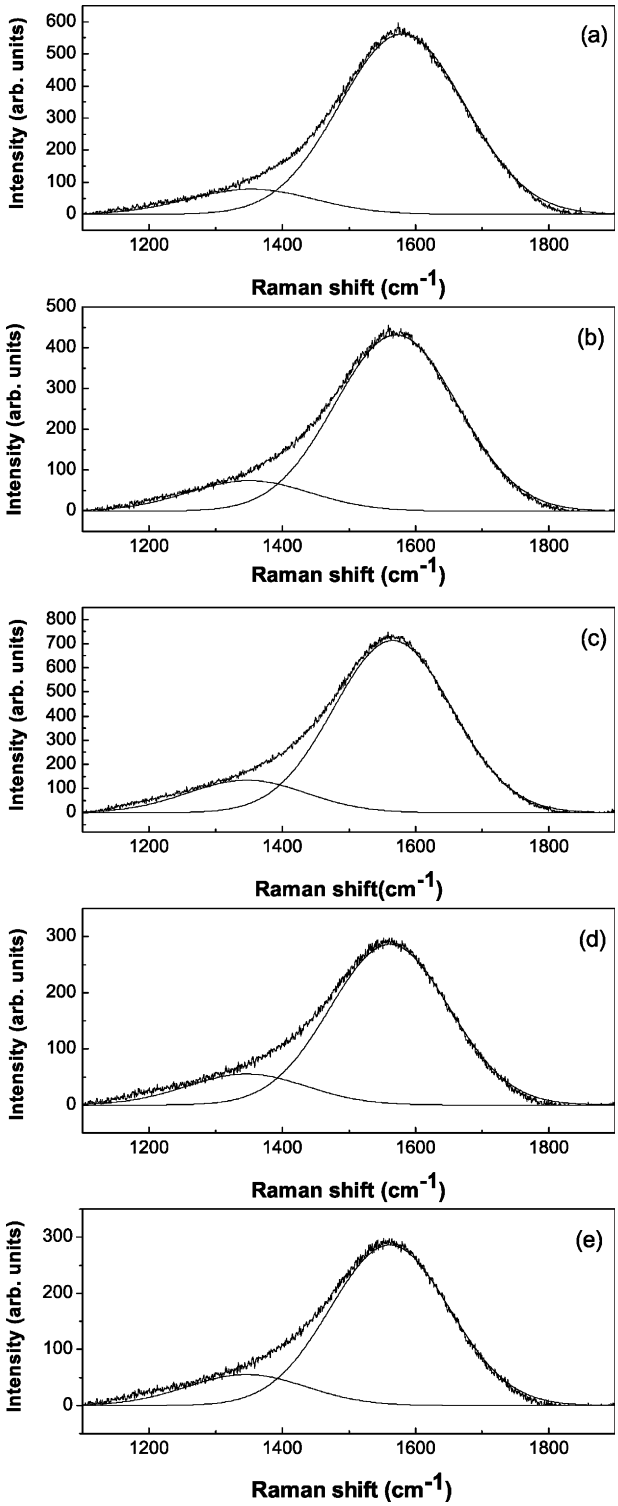

Fig. 2. Gaussian deconvoluted Raman spectra of ta-C:B films with boron content of: (a) 0.59 at.%, (b) 1.65 at.%, (c) 2.13 at.%, (d) 3.51 at.%, (e) 6.04 at.%.

Besides, no other boron-related Raman features were observed in the low-frequency region as those found in some boron doped diamond samples [18]. The line-shape of the Raman spectra is similar to that of B-free ta-C film [19]. To consider the effect of boron on the Raman spectra, it is necessary to compare with the Raman lines of boron carbide (B_4C). The Raman spectrum of B_4C in the high frequency region exhibits a broad band spanning from 1200 to 1700 cm^{-1}, where the 1500–1600 cm^{-1} are for chain-like molecules stretching and the 1260–1420 cm^{-1} for ring-like molecules breathing [20]. This implies that there is little distinction in the G–D region between modes due to C or B. Thus for a network with similar frequency of bond-stretching and ring modes, it is difficult to estimate whether it contains B or not. It is therefore expected little difference between the Raman spectra of boronated and undoped ta-C films in the range of 1100–1900 cm^{-1}. For the sake of simplicity, we analyze the trends in the G and D positions of

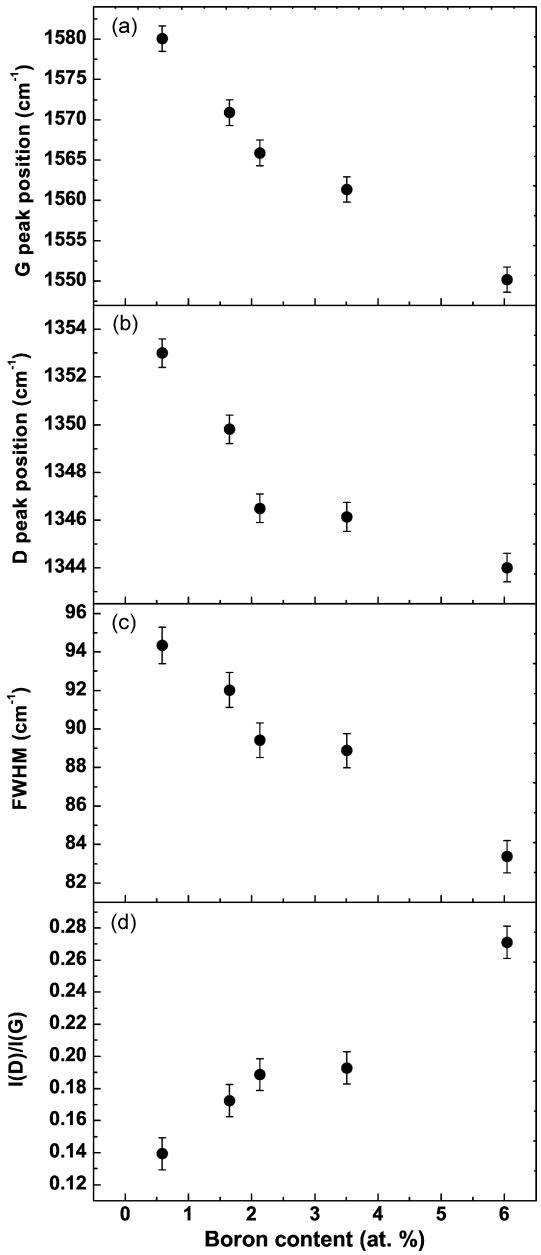

Fig. 3. Variations of Gaussian fitted Raman parameters (a) G peak position, (b) D peak position (c) FWHM of G peak, (d) intensity ratio $I(D)/I(G)$ with boron content in ta-C:B films.

ta-C:B films in the same way as in B-free samples, treating no peaks associated with boron in the Raman spectra for any of the films.

3.3. Gaussian fitting analysis

Empirically, the visible Raman spectra of amorphous carbons (a-C) show one or two prominent features (the G and D bands) and some minor modulations (usually around 1100–1200 and 1400–1500 cm^{-1}) [21]. Since the Raman scattering cross-section for sp^2-bonded material is approximately 40 times higher than that of sp^3-bonded material [22], the analysis of the Raman spectra of ta-C:B should resemble that of a-C. The simplest fit of the spectra consists of two Gaussians, which is shown in Fig. 2. It can be seen that the fitted lines do not deconvolute well with the original curve in the region of 1100–1200 cm^{-1}, indicating a small modulation exists at these low frequencies. The fitted parameters, including G and D band positions, the full width at half maximum (FWHM), and intensity ratios $I(D)/I(G)$, were plotted, respectively, in Fig. 3.

The D band positions of the films are at about 1350 cm^{-1}, and the G positions are around 1565 cm^{-1}. It shows that both the G and D positions shift to lower frequencies with increasing boron content in the films. The D band shift has been stated due to the effect of the sp^2 cluster size [17], as the intensity ratio between D and G bands reflect the change in the size of the sp^2-bonded clusters [23,24]. The high frequency of the G band in ta-C film has been considered to be its high compressive macroscopic stress [25]. However, it was verified that by annealing up to complete stress release only small structure changes were induced in ta-C [26]. Hence the downshift of the G position of ta-C:B films could be explained by a decreased number of oleofinic sp^2 groups in chains. This is just because their vibrational frequencies of G peaks are higher than that of graphite [27].

The FWHMs of D bands almost remain the same for any of the films, but those of G bands gradually become narrower at higher boron concentrations (Fig. 3). Four possible reasons may be responsible for the G line narrowing effects in the films: the cluster size, the cluster distribution, the influence of the stress, and chemical bonding [21]. The change of the line-width of G band results from the removal of strain in bond angel and length which relates to the stress relaxation in ta-C:B film. Sullivan et al. [28] have proposed that an sp^2 site is large than an sp^3 site in the atomic volume but is less in the in-plane size due to shorter bond length. Thus the formation of sp^2 sites with their σ plane aligned in the plane of compression will relieve a biaxial compressive stress [29]. Chhowalla et al. [30] pointed out that boron are predominantly sp^2 hybridized in the ta-C:B film. When a carbon atom has been replaced by B, the local atomic stress relaxed, and the surrounding sp^2 sites will tend to form a large ordered ring. The FWHM versus intrinsic stress of corresponding ta-C:B films is shown in Fig. 4. It can be seen that a stress release of about 5 GPa could reduce the FWHM of G band from 94 to 83 cm^{-1}. The stress of ta-C:B film plays an important role on the variation of the width of G band. On the other hand, the nonlinear relationship between FWHM and stress indicates some other factors exist influencing the line-width of G band.

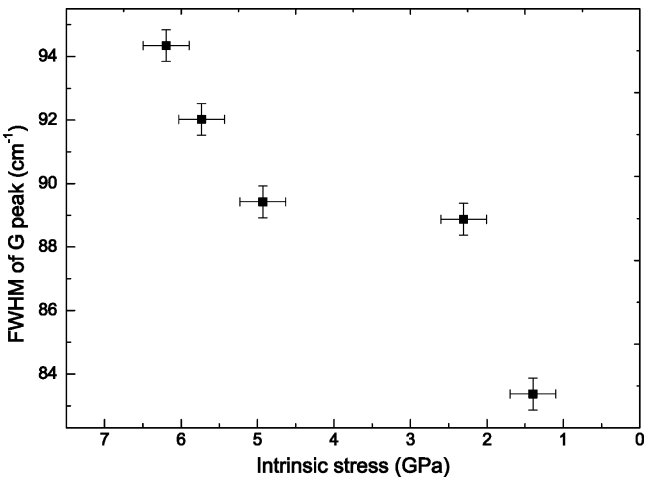

Fig. 4. FWHM of G peak as a function of intrinsic stress.

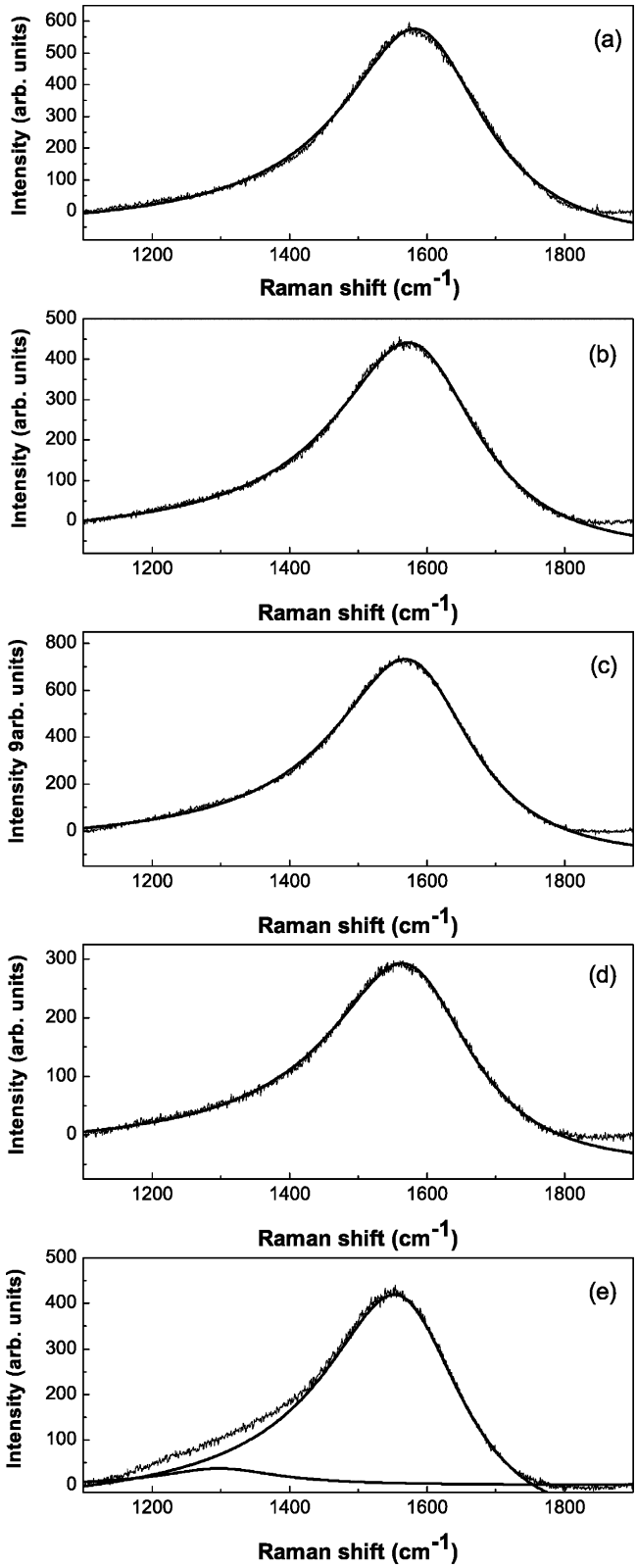

Fig. 5. Raman spectra of ta-C:B films superimposed with a BWF and a Lorentzian line shapes at different boron concentrations: (a) 0.59 at.%, (b) 1.65 at.%, (c) 2.13 at.% (d) 3.51 at.% (e) 6.04 at.%. For the films (a)–(d), a single BWF was sufficient to provide excellent fits to the spectra.

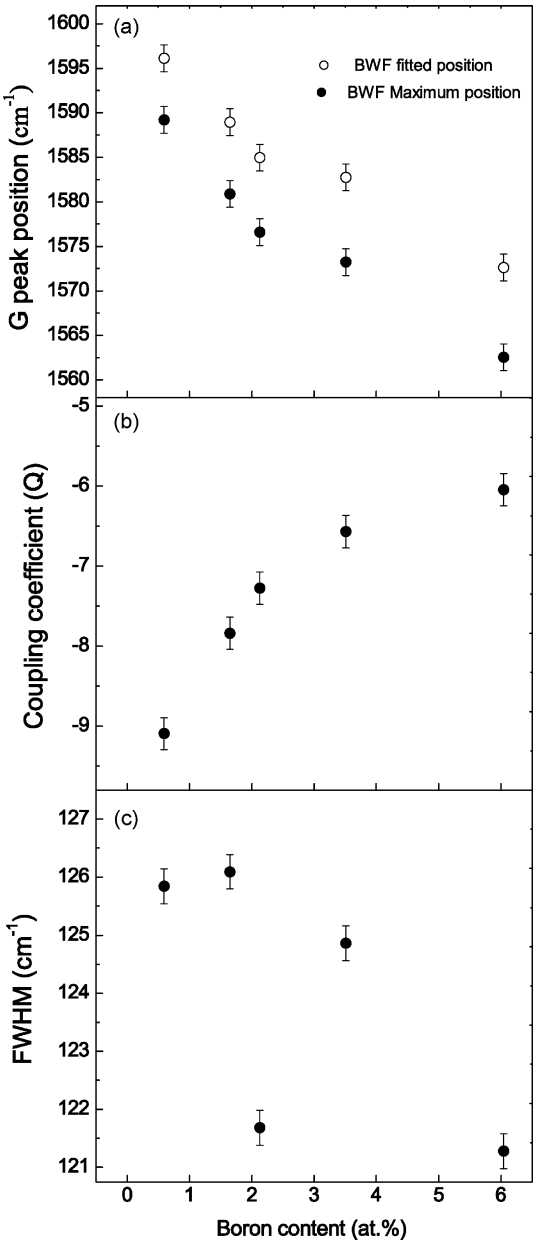

Fig. 6. Variations of BWF fitted Raman parameters (a) G peak position, (b) coupling coefficient and (c) FWHM with the content of boron in ta-C:B films.

For the intensity ratio $I(D)/I(G)$, the result shows an increase from 0.14 to 0.27 as the boron concentration of ta-C:B film rises in magnitude from 0.59 to 6.04 at.%. It has been shown that the intensity ratio $I(D)/I(G)$ can be used as a parameter for sp^3 content [31]. A small value of $I(D)/I(G)$ ratio will correspond to a higher sp^3 content. The major effect of B introduction is to increase the clustering of the sp^2 phase. This has been confirmed from the sp^3 bonding determination of ta-C:B films by XPS in the further work [32]. The sp^3 content of ta-C:B film tended to decrease at high boron concentration. Roy et al. [15] have also studied the effect of excitation wavelength on the magnitude of $I(D)/I(G)$. They reported that the breathing mode was more resonant at high excitation wavelength, whereas the stretching mode dominated at low wavelength. Thus the intensity ratio $I(D)/I(G)$ for the films characterized by 458 nm Raman spectroscopy may be a little lower in our cases due to its shorter excitation wavelength.

3.4. BWF fitting analysis

A widely used fitting method alternative to the Gaussian fit is a Breit–Wigner–Fano (BWF) line for the G band and a Lorentzian for the D band. The BWF line is given as

$$I(\omega) = \frac{I_0[1 + 2(\omega - \omega_0)/Q\Gamma]^2}{1 + [2(\omega - \omega_0)/\Gamma]^2} + a + b\omega$$

where I_0 is the peak intensity, ω_0 the peak position, Γ the FWHM and Q is the coupling coefficient [3,12]. The constants a and b are the corrections for linear background. The BWF line could extend to a low frequency at low Q values, which allows it to account for the different contributions to the Raman spectra. This indicates that it would be more reliable to fit the Raman spectra using the BWF line-shape with respect to Gaussian. On the other hand, as a Lorentzian line-shape is used for the D peak, it would be pushed to lower frequencies due to the wide low-frequency tail of the BWF line with the increase in disorder [12]. So the fit of the D peak and especially its position is the least accurate for quantum analysis.

Fig. 5 shows the Raman spectra decomposed with a BWF line-shape for the same series of ta-C:B films above. A lower frequency of D band is observed due to the dispersion of BWF line. For the Raman spectra of ta-C:B films with boron concentration from 0.59 to 3.51 at.%, shown in Fig. 5(a)–(d), a single BWF was sufficient to provide excellent deconvolutions. The fitted parameters, including G peak position, Q and Γ, are plotted in Fig. 6 as a function of boron content. The shift of G peak position often gives quite opposite trends at varying conditions. This is because the maximum of the BWF line is not at ω_0 but lies at lower frequency $\omega_{max} = \omega_0 + \Gamma/(2Q)$. However, in the case of our ta-C:B films the G fitted position (ω_0) and G peak position (ω_{max}) both shift downward from 1596 to 1572 and from 1589 to 1562 cm^{-1}, respectively (Fig. 6(a)). Although the values of G peak position (ω_{max}) are larger than that obtained using Gaussian deconvolution, the trends of G peak varying with increasing boron content agree well with each other for ta-C:B films. The dispersion of G peak can be also explained by the decreased vibrational contributions of olefinic sp^2 groups.

The parameter Q is a description of the line-shape asymmetry of Raman spectrum. When the boron fraction of the ta-C:B films increased from 0.59 to 6.04 at.%, the coupling coefficient Q increased from −9 to −6 (Fig. 6(b)). The trend of Q versus boron content resembles that of the intensity ratio I(D)/I(G) (Gaussian fit) versus boron content. The magnitudes of the coupling coefficient Q and intensity ratio I(D)/I(G) (Gaussian fit) are both meaningful indicators of the sp^3 content in ta-C:B film. Empirically it is clear that the Q value decreases sharply as the sp^3 fraction increases, and can be used to provide a binary test for films of very high sp^3 content [33]. However, for the intensity ratio I(D)/I(G) (Gaussian fit), it sometimes can be used to quantify the value of sp^3 content in ta-C film [34].

Fig. 6(c) shows the variation of the FWHM of G peak with B content. The G peak width is an indicator of the bond angle distortions in the configuration excited [12]. However, the G width was not seen to decrease or increase with increasing B content.

4. Conclusions

In this study, the surface morphologies and microstructure of ta-C:B films were studied by AFM and Raman spectroscopy. It is shown that the undoped ta-C film contains very fine asperities. While for ta-C:B films, larger clusters and sparser boundaries can be seen at higher boron concentrations. For the analysis of Raman spectra of ta-C:B films, Gaussian line-shape and BWF line-shape were, respectively, used to fit the original curves. The G peak positions obtained from both line shapes were found to shift downward with increasing boron content. The intensity ratio I(D)/I(G) from Gaussian fit and the coupling coefficient from BWF fit both increase as the content of boron increases, indicating a decreased sp^3 content in the ta-C:B films. The FWHM of G peak obtained from Gaussian fit decreases from 94 to 83 cm^{-1} as the boron content changes from 0.59 to 6.04 at.%, implying a distortion removal of bond angle in the ta-C:B films. The reduction of FWHM is a result of stress release in the ta-C:B films. However, the G peak width from BWF fit dose not show an apparent decrease or increase in magnitude with boron concentration varying between 0.59 and 6.04 at.%.

Acknowledgement

The authors are grateful to the National Natural Science Foundation of China (Grant No. 50602012) for financial assistance.

References

[1] J. Robertson, Prog. Solid State Chem. 21 (1991) 199.
[2] J. Robertson, Pure Appl. Chem. 66 (1994) 1789.
[3] J. Robertson, Mater. Sci. Eng. R 37 (2002) 129.
[4] I. Endler, K. Bartsch, A. Leonhardt, Diamond Relat. Mater. 8 (1999) 834.
[5] V.M. Tian, Diamond Relat. Mater. 10 (2001) 153.
[6] J.J. Li, C.Z. Gu, H.Y. Peng, Appl. Surf. Sci. 251 (2005) 236.
[7] X. Yan, T. Xu, G. Chen, Appl. Phys. A 81 (2005) 41.
[8] G.A.J. Amaratunga, V.S. Veerasamy, C.A. Davis, W.I. Milne, et al. J. Non-Cryst. Solids 164–166 (1993) 1119.
[9] C. Ronning, U. Griesmeier, M. Gross, H.C. Hofsass, R.G. Downing, G.P. Lamaze, Diamond Relat. Mater. 4 (1995) 666.
[10] B. Kleinsorge, A. Ilie, M. Chhowalla, W. Fukarek, W.I. Milne, J. Robertson, Diamond Relat. Mater. 7 (1998) 472.
[11] W.I. Milne, Semicond. Sci. Technol. 18 (2003) S81.
[12] A.C. Ferrari, J. Roberson, Phys. Rev. B 61 (2000) 14095.
[13] A.C. Ferrari, Diamond Relat. Mater. 11 (2002) 1053.
[14] Q. Wang, D.D. Allred, L.V. Knight, J. Raman Spectrosc. 26 (1995) 1039.
[15] S.S. Roy, P. Papakonstantinou, R. McCann, G. Abbas, J.P. Quinn, J. McLaughlin, Diamond Relat. Mater. 13 (2004) 1459.
[16] S. Xu, B.K. Tay, H.S. Tan, L. Zhong, Y.Q. Tu, S.R.P. Silva, J. Appl. Phys. 79 (1996) 7239.
[17] E. Liu, X. Shi, B.K. Tay, L.K. Cheah, H.S. Tan, J.R. Shi, Z. Sun, J. Appl. Phys. 86 (1999) 6078.
[18] M. Mermoux, F. Jomard, C. Tavarès, F. Omnès, E. Bustarret, Diamond Relat. Mater. 15 (2006) 572.
[19] J.Q. Zhu, J.C. Han, S.H. Meng, J.H. Wang, W.T. Zheng, Vacuum 72 (2004) 285.
[20] X.Q. Yan, W.J. Li, T. Goto, M.W. Chen, Appl. Phys. Lett. 88 (2006) 131905.
[21] J. Schwan, S. Ulrich, V. Batori, H. Ehrhardt, S.R.P. Silva, J. Appl. Phys. 80 (1996) 440.
[22] D. Papadimitriou, G. Rouparkas, C.A. Dimitriadis, S. Logothetidis, J. Appl. Phys. 92 (2002) 870.
[23] D.G. McCulloch, S. Prawer, A. Hoffman, Phys. Rev. B 50 (1994) 5905.
[24] D.G. McCulloch, S. Prawer, J. Appl. Phys. 78 (1995) 3040.
[25] J.W. Ager, S. Anders, A. Anders, I.G. Brown, Appl. Phys. Lett. 66 (1995) 3444.
[26] A.C. Ferrari, B. Kleinsorge, N.A. Morrison, A. Hart, V. Stolojan, J. Robertson, J. Appl. Phys. 85 (1999) 7191.
[27] G. Irmer, A. Dorner-Reisel, Adv. Eng. Mater. 7 (2005) 694.
[28] J.P. Sullivan, T.A. Friedmann, A.G. Baca, J. Electron. Mater. 26 (1997) 1021.
[29] A.C. Ferrari, S.E. Rodil, J. Robertson, W.I. Milne, Diamond Relat. Mater. 11 (2002) 994.
[30] M. Chhowalla, Y. Yin, G.A.J. Amaratunga, D.R. McKenzie, T. Frauenheim, Appl. Phys. Lett. 69 (1996) 2344.
[31] M.A. Tamor, W.C. Vassell, J. Appl. Phys. 76 (1994) 3823.
[32] J.C. Han, M.L. Tan, J.Q. Zhu, S.H. Meng, B.S. Wang, S.J. Mu, D.W. Cao, Appl. Phys. Lett. 90 (2007) 083508.
[33] K.W.R. Gilkes, S. Prawer, K.W. Nugent, J. Robertson, H.S. Sands, Y. Lifshitz, X. Shi, J. Appl. Phys. 87 (2000) 7283.
[34] B.K. Tay, X. Shi, H.S. Tan, H.S. Yang, Z. Sun, Surf. Coat. Technol. 105 (1998) 155.